

## Extraction Induced by Microemulsion Breaking and Square Wave Voltammetry: A Promising Union to Monitor Cd, Pb and Cu in Biodiesel

Cristian H. Krause,<sup>1b</sup><sup>a</sup> Alexandre B. Schneider,<sup>1b</sup><sup>\*a</sup> Márcia M. da Silva,<sup>a</sup>  
Marina B. Mazzei,<sup>a</sup> Leandro Kolling<sup>1b</sup><sup>a</sup> and Fernando N. Leal<sup>a</sup>

<sup>a</sup>Instituto de Química, Universidade Federal do Rio Grande do Sul, Av. Bento Gonçalves 9500,  
C.P. 15003, 91501-970 Porto Alegre-RS, Brazil

A new approach involving square wave anodic stripping voltammetry was developed to simultaneously determine cadmium and lead and, in the same cell, sequentially copper, in biodiesel after extraction induced by microemulsion breaking. The composition of the water-in-oil microemulsion involved 10.50 mL biodiesel, 4.20 mL *n*-propanol and 0.30 mL of the 6.0 mol L<sup>-1</sup> HNO<sub>3</sub> solution. The extraction was carried out by adding 1.10 mL ultrapure water resulting in two well separated phases: an upper organic phase, and a lower aqueous phase containing the analytes. The apparatus comprised a portable potentiostat and a cell with an *in situ* plated mercury film glassy carbon electrode as working electrode. The limits of detection for Cd, Pb and Cu were 0.33, 0.48 and 0.66 µg L<sup>-1</sup>, respectively. The accuracy of the method was evaluated by recovery assays of spiked samples and by analyzing a standard reference material.

**Keywords:** metals, biodiesel, microemulsion breaking, voltammetry

### Introduction

Biodiesel has several environmental advantages to the conventional diesel originated from fossil sources used in compression-ignition engines, including biodegradability, nontoxic characteristics and the relative absence of sulfur and aromatic compounds. This is an alternative fuel composed of monoalkyl esters from long chain fatty acids, commonly methyl or ethyl esters. Its production occurs mainly from a transesterification reaction between triacylglycerides from renewable resources and a short chain alcohol, such as methanol or ethanol.<sup>1-5</sup>

According to CNPE (National Energy Policy Council), since 2019, diesel oil sold in Brazil must contain at least 11% biodiesel, with this demand increasing 1% *per* year, reaching a minimum of 15% of biodiesel mixed with diesel from 2023 on.<sup>6</sup> This decision contributes to reduce greenhouse gas emissions since this biofuel is derived from renewable resources, such as vegetable oils or animal fats, which are essentially carbon neutral.<sup>7</sup> On the other hand, there is an increasing demand for the evaluation of specifications and quality control of biodiesel.<sup>8</sup> Among these emerging requirements, it is necessary to create

alternative procedures for fast and simple determinations of trace metal such as Cd, Pb and Cu since they are known to interfere with the motor performance,<sup>9</sup> contribute to the formation of gums and sediments in vehicle and fuel tanks,<sup>10</sup> form insoluble salts, induce corrosion and accelerate the deterioration of this biofuel.<sup>1</sup> Moreover, metal contamination affects the biodiesel stability against oxidation<sup>11,12</sup> and the combustion of metal-containing fuels can be a source of pollution, releasing the contaminants Cd and Pb to the atmosphere.<sup>13,14</sup> There is, however, no legislation in Brazil establishing limits for Cd, Pb and Cu in this biofuel.

Different approaches using different analytical techniques, mainly atomic absorption spectrometry (AAS), have been proposed to determine Cd, Pb and Cu and other trace metals in biodiesel using different sample preparation methods.<sup>15-18</sup> On the other hand, square wave anodic stripping voltammetry (SWASV) is one of the most sensitive analytical techniques in the determinations of metals, being a simple and low-cost alternative for this purpose. This technique is based in a previous deposition of the analytes onto the surface of the working electrode (WE) by means of their reductions during the application of a negative potential within a determined period.<sup>19,20</sup> This preconcentration step is followed by stripping the metals off the electrode surface by sweeping potentials normally

\*e-mail: schneider.alexandre@ufrgs.br

Editor handled this article: Rodrigo A. A. Muñoz (Associate)

starting at the deposition potential going to more positive ones, during which positive and negative potential pulses are periodically applied and the current is measured twice, i.e., at the final of the anodic and cathodic pulses.<sup>19-24</sup>

The mercury film electrode (HgFE) is a reliable alternative to the classic hanging mercury drop electrode (HMDE) in voltammetry, due to the less quantity of Hg used.<sup>25</sup> Mercury-film electrode is prepared by coating the WE with a thin film of metallic Hg from a solution containing Hg<sup>II</sup> ions. The plating step can be conducted *ex situ*, i.e., before the analysis, in a separate cell solution containing only Hg<sup>II</sup> ions, or *in situ*, which occurs when Hg<sup>II</sup> is reduced along with the metallic species, both presented in the same solution in the cell.<sup>25</sup> The latter is a faster approach because both, film formation and preconcentration of the analytes occur during one single step. The advantages of the HgFE include a larger surface/volume ratio, mechanical stability, lower mercury consumption, and a very sensitive and selective surface for metals accumulation.<sup>25,26</sup> Therefore, HgFE is widely used with anodic stripping voltammetry (ASV), including the determination of Cd, Pb and Cu in different matrices.<sup>27-32</sup>

Several voltammetric methods to assay Cd, Pb and Cu in biodiesel were proposed in the literature, such as: the simultaneous determination of Pb and Cu by differential pulse anodic stripping voltammetry (DPASV) at a HgFE using microemulsion (ME) as sample preparation,<sup>9</sup> ultrasound-assisted digestion of biodiesel samples for the determination of Zn, Cd, Pb, Cu and Hg by SWASV,<sup>10</sup> the determination of Pb and Cu using ME by SWASV using boron-doped diamond electrode,<sup>33</sup> Cd, Cu, Pb and Zn by SWASV at a bismuth film after microwave digestion with diluted acid and a multivariate optimization,<sup>34</sup> Pb, Cu and Hg with screen-printed gold electrode by SWASV using different batch systems,<sup>35</sup> and the determination of Cu using screen-printed gold electrodes by SWASV using ME.<sup>36</sup>

The direct voltammetric determination in biodiesel using the classic three electrodes setup is not an easy task, because of the high electrical resistivity of the organic matrix.<sup>1</sup> Unless (ultra)microelectrodes are employed as working electrode,<sup>37-40</sup> some previous sample pretreatment must be considered, as cited above. A promising alternative for the extraction of metals from fuels is the extraction induced by microemulsion breaking (EIMB), described by Vicentino and Cassella<sup>41</sup> for the determination of Hg in Brazilian gasoline by cold vapor atomic absorption spectrometry (CVAAS).<sup>41</sup> The EIMB method allowed the determination of Hg in an extracting phase composed of water and *n*-propanol. This is a liquid-liquid extraction method, in which the advantages are the integral partition of the analytes from the sample to the aqueous phase and, additionally, they can

be preconcentrated, since the ratio between the volume of the sample to the extracted phase is normally higher than one.<sup>41</sup> Other studies reported the determination of Cu, Ni, Pb and V in ethanol-containing gasoline by graphite furnace atomic absorption spectrometry (GFAAS),<sup>42</sup> Mg, Mn and Zn in ethyl alcohol-containing gasoline by flame atomic absorption spectrometry (FAAS)<sup>43</sup> and Cd, Mn, Pb and Sb in gasoline by inductively coupled plasma mass spectrometry (ICP-MS),<sup>44</sup> all of them after EIMB. The use of EIMB combined with voltammetric methods was firstly reported for the simultaneous determination of Cd and Pb in gasoline based on an acrylonitrile-butadiene-styrene and a chemically modified bismuth film graphite (AGCE-BiF) working electrode after EIMB.<sup>45</sup>

The extraction of metals to an aqueous phase with a strong electrolyte makes the EIMB a promising and suitable method of sample pretreatment for further voltammetric applications. Hence, this work proposes the simultaneous quantification of traces of Cd and Pb followed by the sequential quantification of traces of Cu in biodiesel samples by SWASV, after EIMB, using low volumes of *n*-propanol and HNO<sub>3</sub> solution during ME formation, and ultrapure water to separate the phases.

## Experimental

### Reagents, solutions, and samples

All chemicals used in the preparation of working solutions were of analytical reagent grade. The ultrapure water was obtained from a Milli-Q system (Millipore, Bedford, USA). Organic standard working solutions, each of them containing Cd, Pb and Cu in the concentration of 2.0 mg kg<sup>-1</sup>, were prepared by diluting their 1000 ppm (Wt.) metallo-organic standards in 20 cSt mineral oil (Conostan, SPC Science, Quebec, Canada) with *n*-propanol (Sigma-Aldrich, St. Louis, USA). White mineral oil (13 cSt) was obtained from Specscol, (Quimlab, Jacareí, Brazil). Inorganic standard working solutions in the concentrations of 10.0 mg L<sup>-1</sup> Cd<sup>II</sup>, Pb<sup>II</sup>, Cu<sup>II</sup>, Ni<sup>II</sup>, Fe<sup>III</sup>, Al<sup>III</sup>, Cr<sup>III</sup>, Cr<sup>VI</sup>, Zn<sup>II</sup>, V<sup>V</sup>, Mo<sup>VI</sup>, Ti<sup>IV</sup>, Te<sup>IV</sup>, Sn<sup>IV</sup>, In<sup>III</sup>, As<sup>III</sup>, U<sup>VI</sup>, Se<sup>IV</sup> and 1.0 mg L<sup>-1</sup> Cd<sup>II</sup>, Pb<sup>II</sup> and Cu<sup>II</sup> were prepared by diluting their 1000 mg L<sup>-1</sup> stock solution (Specsol, Quimlab, Jacareí, Brazil) with ultrapure water and were acidified to 0.1% distilled HNO<sub>3</sub>. The 1000 mg L<sup>-1</sup> Hg<sup>II</sup> inorganic stock solution was obtained from Sigma-Aldrich (St. Louis, USA).

The HNO<sub>3</sub> used in dilutions and in the ME preparations was obtained from Synth (Diadema, Brazil) and further purified by sub-boiling distillation in a quartz sub-boiling distillation system (Kürner Analysentechnik, Rosenheim, Germany). The 1.0 mol L<sup>-1</sup> acetic acid/acetate buffer at

pH 4.6 was prepared by suitable mixing and dilution of 99.7% glacial acetic acid (Dinâmica, Indaiatuba, Brazil) and sodium acetate (Sigma-Aldrich, St. Louis, USA). The biodiesel samples were obtained from independent biodiesel industrial plants located in the Rio Grande do Sul state and were produced mainly from soybean oil.

### Apparatus

Square wave voltammograms were recorded using an EmStat Blue portable potentiostat and the PSTrace software version 5.9 was used for data acquisition (both from PalmSens BV, Houten, The Netherlands). Voltammetric measurements were performed in 5-70 mL conventional borosilicate voltammetric vessels, with a three electrodes setup involving a 3 mm glassy carbon (GC) as WE (Metrohm, Herisau, Switzerland), a platinum bar as counter electrode (CE) and all the potentials were measured against an Ag/AgCl (3 mol L<sup>-1</sup> KCl) reference electrode (RE). A magnetic bar was used to stir the solution by a 728-model magnetic stirrer (Metrohm, Herisau, Switzerland). For the pH measurements, a Kasvi (São José dos Pinhais, Brazil) pH meter was used, which was daily calibrated. The adjustable micropipettes were calibrated at the volumes used.

The plastic materials were left 48 h in a solution containing 10% HNO<sub>3</sub>, 45% ethanol and 45% ultrapure water, followed by a thoroughly rinsing with ultrapure water. The glassware was left 48 h in a 1% HNO<sub>3</sub> solution and then extensively rinsed with ultrapure water.

### Sample preparation: microemulsion formation and breaking

The ME was prepared in a conical polypropylene (PP) flask by adding 10.50 mL of biodiesel sample, 4.20 mL *n*-propanol, and 0.30 mL of the 6.0 mol L<sup>-1</sup> HNO<sub>3</sub> solution under stirring by a magnetic bar. The EIMB was carried out by adding 1.10 mL ultrapure water to the ME, followed by stirring for 15 min, using a magnetic bar. Two well separated phases were then observed, i.e., an organic layer at the top and an aqueous layer at the bottom, to which the analytes were extracted. The organic phase was removed with the aid of a pipette and the whole volume of the aqueous phase extract (APE), i.e., 2.30 mL, was transferred with a micropipette to the cell for further voltammetric measurements.

### Analytical procedure for measurements

The method was applied in a cell containing 2.30 mL of APE (or blank) from the EIMB, 2.70 mL of the

1 mol L<sup>-1</sup> acetic acid/acetate buffer pH 4.6 (final pH in the cell: ca. 4.0) and 50 µL of the 1000 mg L<sup>-1</sup> Hg<sup>II</sup> solution (final concentration in the cell: 10 mg L<sup>-1</sup>). Prior to the determination of the analytes, the GC electrode surface was polished with 0.05 µm alumina slurry (Risitec, São Paulo, Brazil) on a soft and rough pad and washed with ultrapure water.

Afterwards, a deposition potential ( $E_{\text{dep}}$ ) of  $-1.20$  V was set for 200 s deposition time ( $t_{\text{dep}}$ ) under stirring for the simultaneous plating of Cd and Pb, followed by an anodic sweep of the potentials from  $-1.20$  to  $+0.60$  V. Then, two standard additions were made, by adding 50 µL of the inorganic standard working solution, containing both, 1.0 mg L<sup>-1</sup> Cd and 1.0 mg L<sup>-1</sup> Pb, into the cell to evaluate the analytes concentrations by means of the peak current ( $I_p$ ) measurements. Subsequently, the plating of Cu was carried out by setting the  $E_{\text{dep}}$  to  $-0.80$  V for 100 s ( $t_{\text{dep}}$ ) under stirring and the potentials were, then, swept from  $-0.80$  to  $+0.60$  V, followed by two standard additions of 50 µL of the 1.0 mg L<sup>-1</sup> Cu inorganic standard working solution into the cell. Each potential sweep was recorded in triplicate.

The Hg film was generated *in situ* simultaneously with the electroplating of the analytes at every single deposition step. To guarantee reproducible measurements, the potential window comprised the oxidation potential to remove the deposited Hg ( $E_{\text{peak}} = +0.38$  V), going to  $+0.60$  V. A cleaning step ( $E_{\text{clean}}$ ) was also applied between single sample analysis, by keeping the potential at  $+0.60$  V for 30 s. For both, simultaneous and sequential determinations, periodic square wave pulses were applied by setting the frequency ( $f$ ) to 30 Hz, the pulse amplitude ( $\Delta E$ ) to 50 mV and the step potential ( $E_{\text{step}}$ ) to 6 mV. All measurements were conducted at room temperature of  $23 \pm 1$  °C.

The blanks involved a solution resembling the APE, and was prepared by mixing 1.10 mL ultrapure water, 0.90 mL *n*-propanol, and 0.30 mL of the 6.0 mol L<sup>-1</sup> HNO<sub>3</sub> solution, because the APE was constituted of these reagents, as it has been reported.<sup>41-44</sup> The measurements of the blank were carried out according to the analytical procedure described above.

### Accuracy assays

The accuracy of the method was evaluated by recovery assays after spiking different aliquots of one biodiesel sample with Cd, Pb and Cu in three concentration levels and by the analysis of a standard reference material (SRM).

The spikes in 9.5 g biodiesel were carried out prior to the ME formation, where aliquots of the sample were directly added with a determined mass of each metallo-organic standard working solution of Cd, Pb and Cu. For

the analysis of the Standard Reference Material SRM 1084a (wear-metals in lubricating oil), which consist of a blend of metallo-organic compounds in the base oil at nominal levels of  $101 \mu\text{g g}^{-1}$  Pb and  $98 \pm 4 \mu\text{g g}^{-1}$  Cu, a solution was prepared diluting 16.8 mg of the SRM 1084a in 4.2877 g mineral oil. Then, 0.1285, 0.1343, 0.1319, 0.1191 and 0.1307 g of this solution were dissolved in 9.456, 9.459, 9.3986, 9.5732 and 9.629 g biodiesel, respectively, resulting in 5.28, 5.52, 5.46, 4.84 and  $5.28 \mu\text{g kg}^{-1}$  Pb, and 5.13, 5.35, 5.29, 4.69 and  $5.12 \mu\text{g kg}^{-1}$  Cu in biodiesel. Afterwards, each of these aliquots were treated the same way as described in subsections "Sample preparation: microemulsion formation and breaking" and "Analytical procedure for measurements".

## Results and Discussion

### Optimization of the microemulsion formation and breaking

#### Composition of the ME

Homogeneous, transparent, and stable water-in-oil MEs were obtained by mixing biodiesel, *n*-propanol and  $\text{HNO}_3$  solution, containing lower viscosity than the biodiesel sample and lower surface tension between the two immiscible liquids, i.e., biodiesel and  $\text{HNO}_3$  solution.<sup>46-48</sup> The choice of the composition of the ME containing *n*-propanol and  $\text{HNO}_3$  was due to the successful use of these same reagents in a previous work.<sup>15</sup> The ME was rapidly formed using *n*-propanol. Moreover, *n*-propanol has the function of a dispersant agent,<sup>42</sup> which provided a suitable dispersion of the  $\text{HNO}_3$  extractant solution through the biodiesel sample. An important aspect of this composition of the ME is that the addition of surfactant was not necessary, due to the characteristics of biodiesel, which contains a molecular structure like amphiphilic compounds. Hence, the biodiesel itself acts as surfactant in the ME.<sup>49</sup> This behavior of the biodiesel has been assessed in other studies, e.g., as a surfactant additive to reduce heavy oil/bitumen-water interfacial tension in steam assisted recovery processes.<sup>50</sup> In another work, it was discussed that the introduction of biofuel (fatty acid methyl esters) to diesel could result in high levels of polar components, causing an influence in the solvency of the fuel.<sup>51</sup> The ANP (National Agency of Oil, Natural Gas and Biofuels) also describes the action of monoalkyl esters from biodiesel as cleaning solvent for clogged filters.<sup>52</sup>

To obtain the best extraction conditions, four different ME compositions were evaluated, maintaining the volume of  $\text{HNO}_3$  solution constant, and varying the biodiesel/*n*-propanol (B/P) ratio. Different B/P ratio in the ME formation led to the use of distinct water volumes

to cause its breaking, resulting in different volumes of APE. A larger amount of sample (biodiesel) is desirable in the ME composition to increase the concentration of the analytes in the APE. Indeed, the biodiesel content in the ME was kept as high as possible, but more than 70% led to an emulsion formation, as already demonstrated in a ternary diagram for biodiesel/*n*-propanol/ $\text{HNO}_3$  in a previous work.<sup>15</sup> Accordingly, the formation of ME was not observed, possibly due to the low volume of co-surfactant,<sup>41</sup> i.e., *n*-propanol. The B/P ratio of 70/28 was, therefore, chosen, since it kept the ME stabilized and enabled the acquisition of well-defined voltammograms with high  $I_p$  in the APE, as shown in Figure 1. As mentioned before, Antunes *et al.*<sup>15</sup> have already demonstrated that the limits for ME formation was around 75/23, maintaining the content of  $\text{HNO}_3$  solution in 2.0%,<sup>15</sup> which agrees with our results, where homogeneous ME were obtained with a B/P ratio of 70/28. The volume of  $\text{HNO}_3$  solution in the ME was maintained constant to keep the aqueous part of the ME lower than ca. 4% (m/m) and avoid its destabilization, what could lead to an undesirable emulsion formation.<sup>15</sup>

By using a B/P ratio of 70/28, the minimum water volume required for the EIMB was 1.10 mL. Higher volumes of water were required to cause the breaking of other ME compositions with different B/P ratios because a lower content of biodiesel compared to *n*-propanol generated a more stable ME.<sup>15</sup> Moreover, a preconcentration factor of ca. 2.1 in relation to the volume of biodiesel was achieved (10.50 mL biodiesel/5.05 mL of total volume in the cell, including 2.30 mL APE, 2.70 mL filling solution and 50  $\mu\text{L Hg}^{\text{II}}$ ).

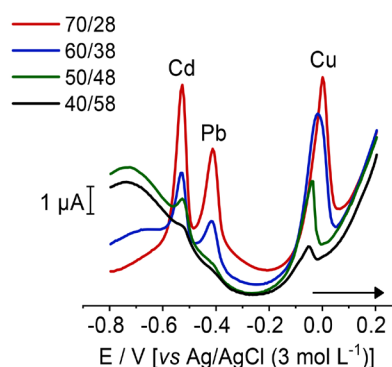


**Figure 1.** Square wave voltammograms in the APE after EIMB with ME containing different B/P ratios. Biodiesel samples spiked with 12, 10 and  $11 \mu\text{g kg}^{-1}$  of Cd, Pb and Cu, respectively.

#### $\text{HNO}_3$ concentration

The effect of different  $\text{HNO}_3$  concentrations in the ME was investigated. This study aimed to identify a suitable  $\text{HNO}_3$  content for the efficient extraction of the analytes from biodiesel since the acid is responsible for the partition

of the metals from the organic phase to the aqueous phase.<sup>41</sup> A total of seven ME aliquots with B/P ratio of 70/28 were prepared containing different  $\text{HNO}_3$  concentrations, varying from 0.04 to 0.28 mol  $\text{L}^{-1}$ .

The  $I_p$  of Cd, Pb and Cu in the APE were plotted against  $\text{HNO}_3$  concentration in the ME (Figure 2), to verify the optimal condition. The height and noise of the baseline and the resolution of the peaks were also evaluated. The ME containing 0.12 mol  $\text{L}^{-1}$   $\text{HNO}_3$  presented a low and smooth baseline and high and well-defined peak shapes, as well as the highest  $I_p$  for Pb and a relatively high  $I_p$  for Cd and Cu. For further measurements, considering the simultaneous and sequential determination in the same cell, a 0.12 mol  $\text{L}^{-1}$   $\text{HNO}_3$  in the ME was applied, which corresponds to 0.30 mL from the 6.0 mol  $\text{L}^{-1}$   $\text{HNO}_3$  stock solution.

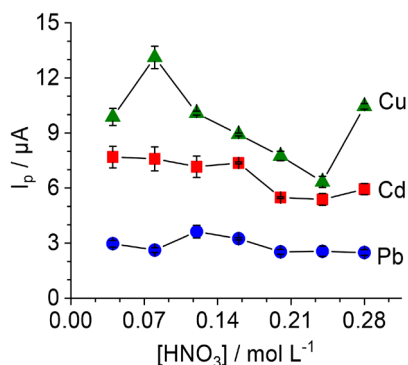


**Figure 2.** Peak currents for Cd, Pb and Cu as a function of  $\text{HNO}_3$  concentration in the ME. Biodiesel samples spiked with 12, 10 and 11  $\mu\text{g kg}^{-1}$  of Cd, Pb and Cu, respectively.

Since the total volume of the APE obtained after the EIMB was 2.30 mL, and we assumed that all the 0.30 mL of 6 mol  $\text{L}^{-1}$   $\text{HNO}_3$  solution and the 1.10 mL of ultrapure water (used for breaking the ME) were contained in the APE, we supposed that the remaining volume (0.90 mL) was due to *n*-propanol, i.e., only part of the *n*-propanol went to the aqueous phase and part remained dissolved in the organic phase due to the characteristics of biodiesel. Therefore, we decided to prepare the blanks by mixing 0.30 mL of 6 mol  $\text{L}^{-1}$   $\text{HNO}_3$ , 1.10 mL of ultrapure water and 0.90 mL *n*-propanol, trying to achieve a composition that resembled the APE.

**Stirring time during the extraction induced by microemulsion breaking**

The stirring time after the addition of ultrapure water during the EIMB was an essential step for the quantitative extraction of the analytes from the organic phase to the APE, because the partition of  $\text{Cd}^{\text{II}}$ ,  $\text{Pb}^{\text{II}}$  and  $\text{Cu}^{\text{II}}$  depends on the contact time between the two phases.<sup>41</sup> The magnetic stirrer was set to 800 rpm and as can be seen in Figure 3,

low recoveries values were observed for stirring times below 10 min. Recoveries of  $95 \pm 9$ ,  $94 \pm 8$  and  $86 \pm 7\%$  were obtained for Cd, Pb and Cu, respectively, after 15 min stirring time, which was chosen as the best condition for the extraction.

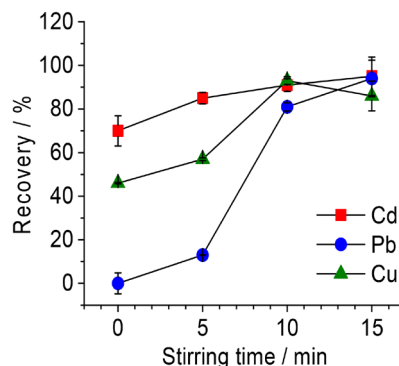


**Figure 3.** Recoveries for 2.95  $\mu\text{g kg}^{-1}$  Cd, 2.00  $\mu\text{g kg}^{-1}$  Pb and 2.40  $\mu\text{g kg}^{-1}$  Cu in biodiesel with different stirring times during the EIMB. Stirring speed: 800 rpm.

**Optimization of the experimental parameters**

**Composition of the solution in the cell**

Different filling solutions (FS) were tested to reach the minimum volume of 5 mL required for the measurements, i.e., 2.30 mL APE plus 2.70 mL FS. By adding 2.70 mL of 0.50 mol  $\text{L}^{-1}$   $\text{HNO}_3$ , i.e., a more acidic medium, an increase of the baseline was verified and only the Cu peak appeared, which could be explained by an increased generation of  $\text{H}_2$  during the deposition step, greatly affecting the deposition of Cd and Pb. Moreover, another unknown signal arose at a potential ca. 0.2 V more negative than the Cu peak potential. In contrast to this, when only ultrapure water was evaluated as FS, a lower baseline was observed. However, no Cd and Pb signals were observed again, and the Cu peak decreased considerably, and we suppose that this is because there was no extra addition of ions to the supporting electrolyte but, on the contrary, the electrolyte coming from the APE (basically  $\text{HNO}_3$ ) was only diluted, which reduced the conductivity of the solution, leading to a lower efficiency in the reduction of Cd, Pb and Cu ions. Only when an aliquot of the 1.0 mol  $\text{L}^{-1}$  acetic acid/acetate buffer solution at pH 4.6 was employed, the Cd and Pb peaks became visible. Moreover, the Cu peak was the highest compared to the other evaluated FS, indicating that the final pH of the solution in the cell (around 4.0) was the most favorable, what was also reported before.<sup>30,53</sup>

**In situ formation of the Hg film**

The Hg film glassy carbon electrode (HgGCE) plays an important role in the determination of Cd, Pb and Cu

by ASV in different matrices,<sup>9,27,28,53</sup> because of a series of advantages such as mechanical stability, larger surface/volume ratio, and the minimum consumption of Hg.<sup>25,26</sup> The *in situ* formation of the HgGCE was another advantage of the method since it enabled the film formation and the metal preconcentration in one step, decreasing the time of analysis and the risk of external contamination. The Hg was removed from the surface of the GCE after each potential sweep, by opening the potential window beyond the Hg<sup>II</sup> oxidation peak potential, i.e., scanning until +0.60 V. After each sample analysis, an additional cleaning step was applied by maintaining the potential at +0.60 V for 30 s, to guarantee the complete removal of everything that could remain deposited on the electrode.

An appreciable increase in  $I_p$  for all analytes was observed using 9.0 and 10.0 mg L<sup>-1</sup> Hg<sup>II</sup> (Figure 4a). In this study, a Hg<sup>II</sup> concentration of 10.0 mg L<sup>-1</sup> was chosen, to ensure that the film formation between measurements was reproducible. In the literature, lower and higher Hg concentrations than in our work were used.<sup>9,28,29,32</sup>

#### The sequential determination

The simultaneous determination of Cd, Pb and Cu, evidenced by the poor coefficient of determination ( $R^2$ ) for all three analytes, was not possible to be carried out, probably due to the mutual interference during the deposition step or the undesirable formation of metal alloys onto the WE surface. The sequential Cu determination, however, was possible to be conducted in the same cell after the simultaneous Cd and Pb determination since their concentrations remained constant during the acquisition of the Cu signals and during standard additions.

The  $E_{dep}$  at which the analytes were deposited onto the surface of the WE, at the same time as the Hg film formation, was evaluated. In ASV, the preconcentration step affects the sensitivity of the method.<sup>20,24</sup> The more negative the potential, the more favorable was the deposition of Cd and Pb, as verified by their increasing  $I_p$  measured during the anodic stripping (Figure 4b). At an  $E_{dep}$  of -1.40 V, the mean  $I_p$  of Pb seemed to slightly decrease, which characterizes the competitive reduction of hydrogen ions presented in solution.<sup>24</sup> Therefore, the  $E_{dep}$  of -1.20 V was chosen as a safe potential for Cd and Pb deposition, to prevent the potential interference that may be caused by hydrogen ions.

The  $E_{dep}$  of -1.40 V presented the highest  $I_p$  for Cu. Nevertheless, the trend of changes in its  $I_p$  versus  $E_{dep}$  was somewhat different from the Cd and Pb ones, presenting a nonlinear variation between -0.80 and -1.40 V (Figure 4b). This nonlinear behavior probably happened because, at more negative potentials, there was a higher tendency for

metal alloys formation onto the working electrode surface among Cu and other metals also presented in solution.<sup>24,54-56</sup> By applying an  $E_{dep}$  of -0.80 V, we suppose that this interference caused by alloys formation did not occur. Hence, the  $E_{dep}$  of -0.80 V was chosen for the sequential determination of Cu. In fact, during the standard addition calibration, a higher coefficient of determination ( $R^2$ ) was obtained by using this condition.

As expected, the longer  $t_{dep}$  the solution in the cell was kept at -1.20 V (under constant stirring), the higher the amount of Cd<sup>II</sup> and Pb<sup>II</sup> reduced and plated on the HgGCE. For further developments, a  $t_{dep}$  of 200 s was chosen for simultaneous Cd and Pb determination and a  $t_{dep}$  of 100 s for the sequential Cu determination since their concentrations from real biodiesel samples are expected to be in the range of low  $\mu\text{g L}^{-1}$  in the APE after EIMB and during the standard additions. If a higher sensitivity is required, the  $t_{dep}$  could be increased. On the other hand, if the biodiesel carries a relatively high content of the analytes, then either the  $t_{dep}$  could be decreased or a higher dilution of the APE in the solution contained in the cell could be applied, to guarantee a linear standard addition calibration curve.

The  $\Delta E$  of the applied square wave pulses, as well as the  $E_{step}$  of the potential-time profile on which the pulses were superimposed, were also evaluated (Figures 4c and 4d). As can be seen, higher pulse amplitudes up to 50 mV caused the increase of  $I_p$  for all three analytes. At higher  $\Delta E$  than 50 mV, there was a broadening of the peaks as well as an increase in the height of the baseline, what is expected, because there is no time enough for the capacitive current to decay sufficiently,<sup>57</sup> even though the currents are sampled only at the end of both, the cathodic and anodic pulses. Regarding the  $E_{step}$  for the potential-time modulation signal, the higher its value, the higher the  $I_p$  of Cd, Pb and Cu (Figure 4d), but from 7 mV on the resolution of the signals started being impaired, generating square-shaped signals, i.e., non-gaussian peaks. Then, an  $E_{step}$  of 6 mV and an  $\Delta E$  of 50 mV were chosen for further measurements.

The  $f$  of the applied square wave pulses was also evaluated, and the chosen value was 30 Hz, which enabled the acquisition of well-defined peaks with relatively high  $I_p$  for Cd, Pb and Cu. Frequencies higher than 30 Hz resulted in noisy voltammograms, impairing the correct and reproducible evaluation of the peaks.

#### Study of interferences

The presence of other metals in biodiesel, including Ni<sup>II</sup>, Fe<sup>III</sup>, Al<sup>III</sup>, Cr<sup>III</sup> and Cr<sup>VI</sup> may also occur due to the production process, contact with distillation equipment, storage or transport.<sup>17</sup> Moreover, metals could be present

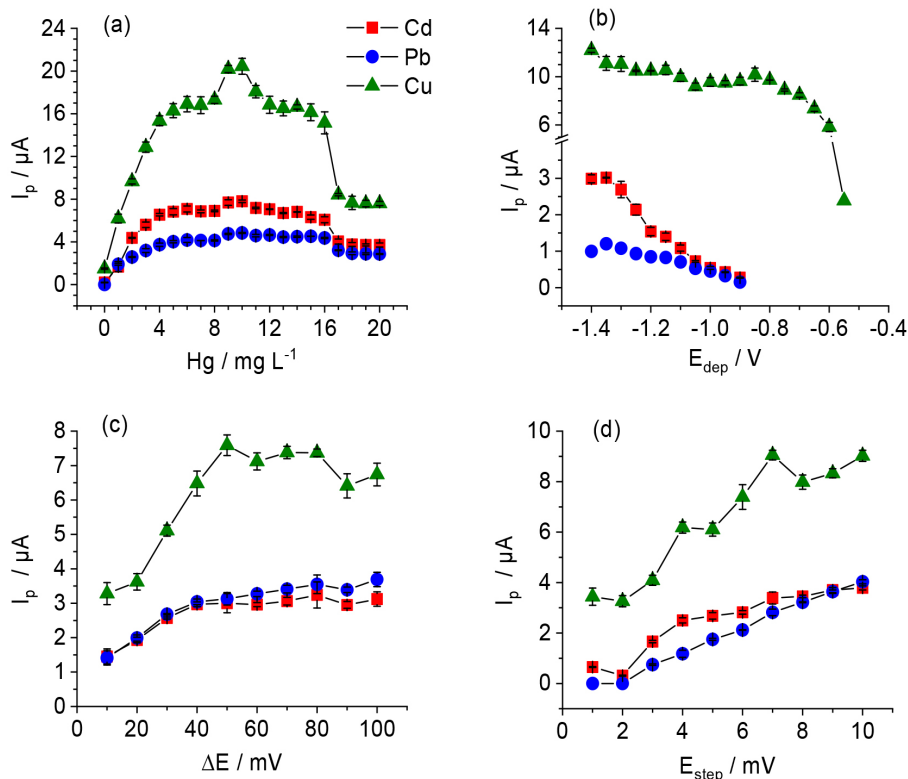


**Figure 4.** Peak currents of  $50 \mu\text{g L}^{-1}$  Cd, Pb and Cu as a function of: (a)  $\text{Hg}^{\text{II}}$  concentration, (b)  $E_{\text{dep}}$ , (c)  $\Delta E$  and (d)  $E_{\text{step}}$  in the solution in the cell containing the APE after EIMB. For (a) to (d): 2.30 mL APE and 2.70 mL of  $1.0 \text{ mol L}^{-1}$  acetic acid/acetate buffer pH 4.6.

in vegetable oils coming from seeds, due to the availability of metals in the soil from pesticides and fertilizers.<sup>58,59</sup> The metals cited above as well as other elements like  $\text{Zn}^{\text{II}}$ ,  $\text{V}^{\text{V}}$ ,  $\text{Mo}^{\text{VI}}$ ,  $\text{Ti}^{\text{IV}}$ ,  $\text{Te}^{\text{IV}}$ ,  $\text{Sn}^{\text{IV}}$ ,  $\text{In}^{\text{III}}$ ,  $\text{As}^{\text{III}}$ ,  $\text{U}^{\text{VI}}$  and  $\text{Se}^{\text{IV}}$  can be determined using the HgGCE as WE,<sup>29,60-72</sup> although for many of them the determination is only possible in the presence of specific ligands and after applying adsorptive stripping voltammetry with a cathodic potential sweep. It is, therefore, important to assess the possible interference caused by them on the voltammograms of Cd, Pb and Cu since they could interact with the Hg film and appear in the potential window during the stripping step. This study was carried out by verifying the influence on  $50 \mu\text{g L}^{-1}$  Cd, Pb and Cu by all the species cited above varying its concentrations in 50, 100 and  $150 \mu\text{g L}^{-1}$ , i.e., reaching the ratios interfering species to analytes of 1:1, 2:1 and 3:1. Each measurement was carried out in triplicate.

Most of the species up to  $150 \mu\text{g L}^{-1}$  did not significantly interfere on the  $I_p$  of the three analytes and did not overlap their peaks. Molybdenum(VI) at the ratios 1:1, 2:1 and 3:1 caused the  $I_p$  of Cd to decrease 15, 16 and 24%, respectively, but had an appreciable negative effect on the Pb peak only at the ratio 3:1, i.e.,  $-20\%$  ( $-1$  and  $-6\%$  at 1:1 and 2:1, respectively). This could have happened because of competitive deposition of the interfering species or formation of intermetallic compounds, during the

deposition step, causing lower sensitivity.<sup>25</sup> Vanadium(V) and  $\text{Te}^{\text{IV}}$  also had a significant influence on decreasing the peaks of Cd, Pb and Cu, with  $\text{Te}^{\text{IV}}$  having an additional effect of causing the appearance of a shoulder partially overlapping the Cu peak. Indium(III) also caused the appearance of a small shoulder on the peak of Cu. Tin(IV) caused an important decrease in the peak height of all analytes but only at the ratio 3:1, what was also the case of  $\text{Fe}^{\text{III}}$ .

Molybdenum(VI) also affected the Cu peak, but increasing its height, i.e., 15, 10 and 14% at 1:1, 2:1 and 3:1, respectively. Selenium(IV), on the other hand, increased the  $I_p$  of Cd and Pb, but not the  $I_p$  of Cu, by ca. 30 and 45%, respectively, independently of the ratio to the analyte and that could be due to the formation of a synergic film layer on the WE, since Se was previously used as a film electrode.<sup>73</sup> Chromium(III) also presented a similar effect on the Cu peak, increasing its  $I_p$  by 8, 15 and 36% at the ratios 1:1, 2:1 and 3:1, respectively. It is worth to mention that none of all those species alone presented any peak at the peak potentials of the analytes during the anodic stripping. Moreover, if they would eventually occur in the biodiesel sample, its concentrations in the APE would remain constant during the measurements, being considered as part of the matrix, and every negative or positive effect that they may have on the signals of Cd, Pb and Cu would be

masked by the standard addition method since the analyte added would suffer the same effect of the analyte already contained in the sample.

#### Analytical characteristics

##### Calibration curves and LOD

The calibration curves and limits of detection (LOD) for Cd, Pb and Cu are showed in Table 1 and were obtained under the optimized conditions. The calibration curves were linear ( $R^2 > 0.991$ ) from 4.9 to 112  $\mu\text{g L}^{-1}$  for Cd, from 4.9 to 112  $\mu\text{g L}^{-1}$  for Pb and from 4.9 to 250  $\mu\text{g L}^{-1}$  for Cu (Figure 5), and then, the  $I_p$  stopped increasing linearly. Table 2 shows the relatively wide linear range comprising low to

intermediate ppb levels found here, which is satisfactory, compared to other works. The values of LOD were calculated following the  $3a/s$  criteria,<sup>74</sup> where  $a$  refers to the standard deviation of the intercept of the standard addition calibration curve ( $n = 6$ ) and  $s$  is the corresponding slope.

##### Accuracy

Table 3 presents the results of recovery assays for three aliquots of a biodiesel sample spiked with three different Cd, Pb and Cu concentrations. Recoveries lay between 86 and 102% for Cd, 94 and 109% for Pb and 89 and 106% for Cu. For this low concentration level, recovery values agreed with the Brazilian guideline orientation about validation of analytical methods.<sup>75</sup> Figure 6 shows the square wave

**Table 1.** SWASV calibration curves for Cd, Pb and Cu in the APE after ME breaking with *in situ* modified HgGCE using the optimized conditions

Analyte	$E_{\text{dep}} / \text{V}$	$t_{\text{dep}} / \text{s}$	Slope / ( $\mu\text{A } \mu\text{g L}^{-1}$ )	Intercept	$R^2$	LOD / ( $\mu\text{g L}^{-1}$ )
Cd	-1.20	200	$0.146 \pm 0.002$	$0.14 \pm 0.02$	0.999	0.33
Pb	-1.20	200	$0.062 \pm 0.001$	$1.2 \pm 0.0$	0.999	0.48
Cu	-0.80	$0.088 \pm 0.002$	$1.1 \pm 0.0$	0.999	0.66	

$E_{\text{dep}}$ : deposition potential;  $t_{\text{dep}}$ : deposition time; LOD: limit of detection;  $R^2$ : coefficient of determination.

**Table 2.** Comparison of the linear range of the developed method with other approaches to determine Cd, Pb and Cu in biodiesel by voltammetry

Electrode	Sample treatment	Linear range / ( $\mu\text{g L}^{-1}$ )			Reference
		Cd	Pb	Cu	
HgGCE	microemulsion	–	4.14-20.72	1.27-6.35	9
HgGCE	US-assisted digestion	0-150	0-160	0-320	10
BDD	microemulsion	–	6.22-37.30	1.91-11.44	33
BiGCE	MW digestion	0.2-80	0.4-80	0.1-100	34
SPGE	USB digestion	–	20-280	20-280	35
HgGCE	EIMB	4.9-112	4.9-112	4.9-250	this work

HgGCE: mercury film glassy carbon electrode; US: ultrasound; BDD: boron-doped diamond electrode; BiGCE: bismuth film glassy carbon electrode; MW: microwave; SPGE: screen-printed gold electrode; USB: ultrasonic bath; EIMB: extraction induced by microemulsion breaking.

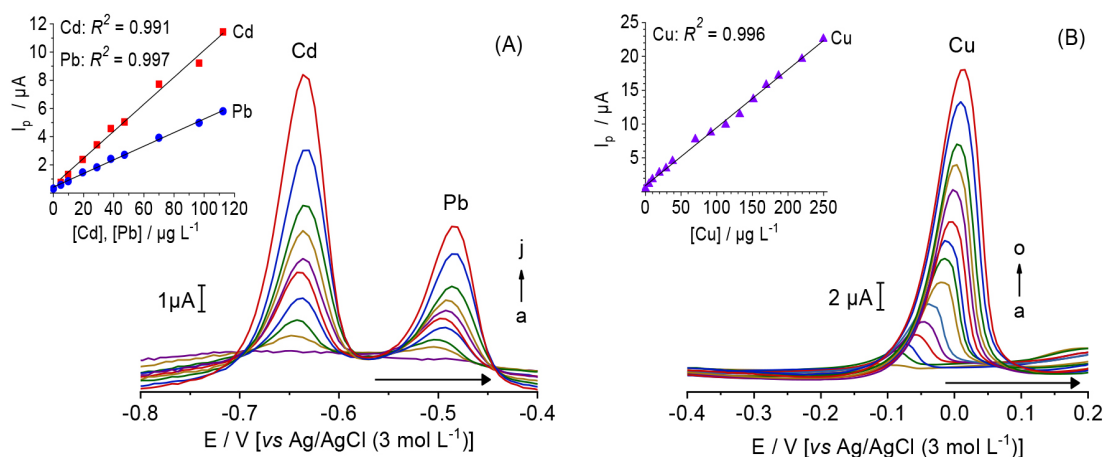


**Figure 5.** Square wave voltammograms for successive standard additions of (A) Cd, Pb and (B) Cu. In the cell: 2.30 mL of APE, 2.70 mL of 1.0 mol  $\text{L}^{-1}$  acetic acid/acetate buffer pH 4.6, 10 mg  $\text{L}^{-1}$  Hg, pH 4.0. (A) (a to j): 4.9 to 112  $\mu\text{g L}^{-1}$  Cd and Pb.  $E_{\text{dep}}$ : -1.20 V,  $t_{\text{dep}}$ : 200 s,  $f$ : 30 Hz,  $\Delta E$ : 50 mV,  $E_{\text{step}}$ : 6 mV. (B) (a to o): 4.9 to 250  $\mu\text{g L}^{-1}$  Cu.  $E_{\text{dep}}$ : -0.80 V,  $t_{\text{dep}}$ : 100 s,  $f$ : 30 Hz,  $\Delta E$ : 50 mV,  $E_{\text{step}}$ : 6 mV.

**Table 3.** Recoveries for Cd, Pb and Cu in the APE after EIMB

		Aliquot 1		Aliquot 2		Aliquot 3	
Added concentration / ( $\mu\text{g kg}^{-1}$ )		0	2.6	0	4.8	0	7.4
Found concentration / ( $\mu\text{g kg}^{-1}$ )	Cd	$0.56 \pm 0.06$	$2.8 \pm 0.3$	$0.56 \pm 0.06$	$5.2 \pm 0.2$	$0.56 \pm 0.06$	$8.1 \pm 0.7$
Recovery / %		–	86	–	97	–	102
Added concentration / ( $\mu\text{g kg}^{-1}$ )		0	2.2	0	4.5	0	7.0
Found concentration / ( $\mu\text{g kg}^{-1}$ )	Pb	$2.3 \pm 0.2$	$4.7 \pm 0.5$	$2.3 \pm 0.2$	$6.8 \pm 0.6$	$2.3 \pm 0.2$	$8.9 \pm 0.9$
Recovery / %		–	109	–	100	–	94
Added concentration / ( $\mu\text{g kg}^{-1}$ )		0	2.6	0	5.2	0	8.2
Found concentration / ( $\mu\text{g kg}^{-1}$ )	Cu	0	$2.5 \pm 0.1$	0	$5.5 \pm 0.6$	0	$7.3 \pm 0.0$
Recovery / %		–	96	–	106	–	89

voltammograms for  $3.11 \mu\text{g kg}^{-1}$  Cd,  $7.54 \mu\text{g kg}^{-1}$  Pb and  $4.57 \mu\text{g kg}^{-1}$  Cu (aliquot 1 in Table 3).

Since there is no reference material for biodiesel that is certified for Cd, Pb and Cu, the Standard Reference Material SRM 1084a (wear-metals in lubricating oil) was used to evaluate the accuracy. Due to the high level of the analytes in the SRM, small amounts of this material were dissolved in biodiesel sample aliquots, as described before (subsection “Accuracy assays”). Thus, the quantity of the SRM 1084a added to the sample was not enough to make considerable changes in the matrix of the biodiesel. Table 4 presents the recoveries of Pb and Cu in the SRM. Recoveries varied between 82 and 108% for Pb and 88 and

104% for Cu. The values found for Pb and Cu in the SRM did not significantly differ from the values indicated in the certificate, according to the Student’s *t*-test, at a significance level of 0.05.

#### Real sample analysis

The validated method was applied in biodiesel samples (Table 5). Surprisingly, Cd was found in most of the samples in the range of  $0.4$  to  $0.6 \mu\text{g kg}^{-1}$ , although it is very low. It is worth to mention that it is possible to quantify very low concentrations of Cd in the cell since it has the lowest LOD among the analytes investigated here. Two samples also

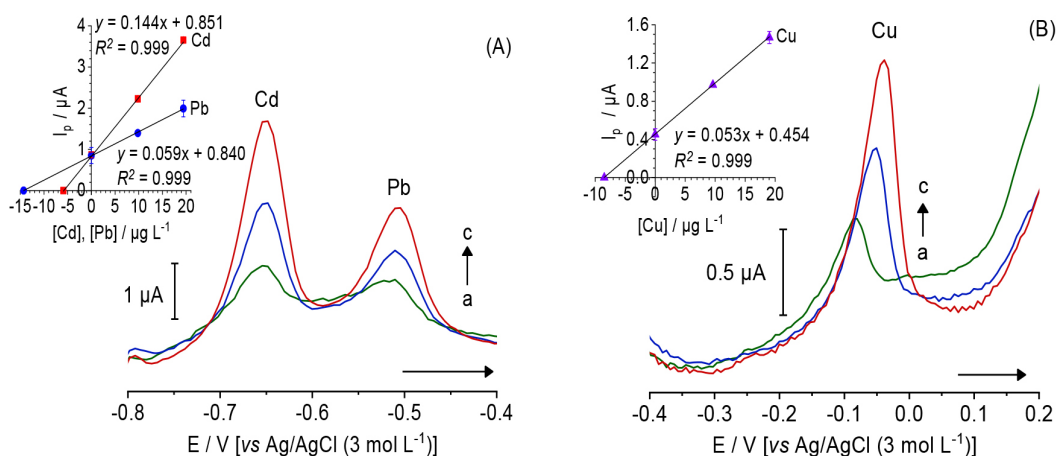


**Figure 6.** Square wave voltammograms for Cd, Pb and Cu. In the cell: 2.30 mL of APE, 2.70 mL of  $1.0 \text{ mol L}^{-1}$  acetic acid/acetate buffer pH 4.6 and  $10.0 \text{ mg L}^{-1} \text{ Hg}^{\text{II}}$ . (A)  $E_{\text{dep}}: -1.20 \text{ V}$ ,  $t_{\text{dep}}: 200 \text{ s}$ . Standard additions for Cd and Pb, (a to c): sample,  $+ 9.8 \mu\text{g L}^{-1}$ ,  $+ 19.4 \mu\text{g L}^{-1}$ . (B)  $E_{\text{dep}}: -0.80 \text{ V}$ ,  $t_{\text{dep}}: 100 \text{ s}$ . Standard additions for Cu, (a to c): sample,  $+ 9.6 \mu\text{g L}^{-1}$ ,  $+ 19.0 \mu\text{g L}^{-1}$ . For (A) and (B),  $f: 30 \text{ Hz}$ ,  $\Delta E: 50 \text{ mV}$ ,  $E_{\text{step}}: 6 \text{ mV}$ . The upper left graphs show the standard addition calibration curves.

**Table 4.** Determination of Pb and Cu in SRM 1084a for evaluation of the accuracy of the developed method

	Certified			Found		
Pb / ( $\mu\text{g g}^{-1}$ )	$101 \pm 1$	$109 \pm 8$	$83 \pm 2$	$90 \pm 2$	$98 \pm 10$	$91 \pm 2$
Agreement / %	–	108	82	89	97	90
Cu / ( $\mu\text{g g}^{-1}$ )	$98 \pm 4$	$99 \pm 2$	$87 \pm 6$	$86 \pm 0.4$	$102 \pm 9$	$100 \pm 3$
Agreement / %	–	101	89	88	104	102

**Table 5.** Application of the optimized and validated method in biodiesel samples

Sample	Biomass	Cd / ( $\mu\text{g kg}^{-1}$ )	Pb / ( $\mu\text{g kg}^{-1}$ )	Cu / ( $\mu\text{g kg}^{-1}$ )
A	100% soybean	$0.56 \pm 0.06$	$2.30 \pm 0.23$	ND
B	83% soybean and 17% animal fat	$0.29 \pm 0.04$	ND	ND
C	99.71% soybean and 0.29% animal fat	$0.09 \pm 0.01$	$2.17 \pm 0.14$	ND
D	100% soybean	ND	ND	ND
E	100% soybean	$0.37 \pm 0.01$	ND	ND

Blank corrected values; ND: not detected.

presented ca.  $2 \mu\text{g kg}^{-1}$  Pb. The presence of these metals in biodiesel may occur due to the production process, contact with distillation equipment, storage or transport.<sup>17</sup> Moreover, metals could enter the soil from pesticides and fertilizers<sup>58,59</sup> and accumulate in seeds and then, in vegetable oils. Concentrations of Cu were below LOD in all samples analyzed here.

## Conclusions

An alternative method for simultaneous determination of Cd, Pb and sequential determination of Cu in biodiesel was presented, based on square wave anodic stripping voltammetry after EIMB, using low volumes of *n*-propanol and  $\text{HNO}_3$  solution to form the microemulsion than found in the literature, and ultrapure water to separate the phases. The stirring time during the EIMB proved to be an important factor to extract the analytes quantitatively to the aqueous phase. The ability to determine Cd, Pb and Cu using EIMB is an important achievement in comparison with other more sophisticated sample preparation methods. The method proved to be accurate, and low LODs and wide linear ranges were achieved. Moreover, this is a low-cost approach to evaluate those metals in commercial biodiesel samples, involving a simpler sample pretreatment and the possibility to carry out the determinations in a decentralized way, since the method demanded a miniaturized instrumentation, with a portable potentiostat and a notebook to data acquisition. The union of EIMB and square wave anodic stripping voltammetry showed to be an interesting alternative to quantify low concentrations of Cd, Pb and Cu in biodiesel, overcoming the problems that arise at the application of this voltammetric technique directly to the biodiesel matrix or the microemulsion, using the classic three electrodes setup.

## Acknowledgments

We thank the Coordination for the Improvement of Higher Education Personnel (CAPES - Finance Code 001) for the financial support (grant No.88887.496090/2020-

00). M.M.S. and L.K. thank for the research scholarships from CNPq (grant No. 311269/2019-2) and CAPES (grant No. 88887.474187/2020-00), respectively. The authors also thank the Center of Fuels, Biofuels, Lubricants e Oils (CECOM-UFRGS) for all the support given during the executions of the experiments, and local biodiesel manufacturer companies for having provided the biodiesel samples.

## Author Contributions

Cristian H. Krause was responsible for conceptualization, data curation, investigation, validation, visualization, writing original draft, writing-review and editing; Alexandre B. Schneider for conceptualization, data curation, project administration, validation, writing-review and editing; Márcia M. da Silva for conceptualization, project administration, validation, writing-review and editing; Marinha B. Mazzei for investigation; Leandro Kolling for writing-review and editing; Fernando N. Leal for investigation.

## References

- Santos, A. L.; Takeuchi, R. M.; Muñoz, R. A. A.; Angnes, L.; Stradiotto, N. R.; *Electroanalysis* **2012**, *24*, 1681. [Crossref]
- Issariyakul, T.; Dalai, A. K.; *Renewable Sustainable Energy Rev.* **2014**, *31*, 446. [Crossref]
- Saluja, R. K.; Kumar, V.; Sham, R.; *Renewable Sustainable Energy Rev.* **2016**, *62*, 866. [Crossref]
- Knothe, G.; Razon, L. F.; *Prog. Energy Combust. Sci.* **2017**, *58*, 36. [Crossref]
- Gebremariam, S. N.; Marchetti, J. M.; *Energy Convers. Manage.* **2018**, *168*, 74. [Crossref]
- Conselho Nacional de Política Energética (CNPE); Resolução No. 16, de 29 de outubro de 2018, Dispõe sobre *A Evolução da Adição Obrigatória de Biodiesel ao Óleo Diesel Vendido ao Consumidor Final, em Qualquer Parte do Território Nacional*; Diário Oficial da União (DOU), Brasília, No. 215, de 08/11/2018, p. 2. [Link] accessed in November 2022
- Cremones, P. A.; Feroldi, M.; Nadaleti, W. C.; de Rossi, E.; Feiden, A.; de Camargo, M. P.; Cremones, F. E.; Klajn, F. F.; *Renewable Sustainable Energy Rev.* **2015**, *42*, 415. [Crossref]

8. Hassan, M. H.; Kalam, M. A.; *Procedia Eng.* **2013**, *56*, 39. [Crossref]
9. Martiniano, L. C.; Abrantes, V. R.; Neto, S. Y.; Marques, E. P.; Fonseca, T. C. O.; Paim, L. L.; Souza, A. G.; Stradiotto, N. R.; Aucélio, R. Q.; Cavalcante, G. H. R.; *Fuel* **2013**, *103*, 1164. [Crossref]
10. Freitas, H. C.; Almeida, E. S.; Tormin, T. F.; Richter, E. M.; Munoz, R. A. A.; *Anal. Methods* **2015**, *7*, 7170. [Crossref]
11. Yaakob, Z.; Narayanan, B. N.; Padikkaparambil, S.; *Renewable Sustainable Energy Rev.* **2014**, *35*, 136. [Crossref]
12. Sundus, F.; Fazal, M. A.; Masjuki, H. H.; *Renewable Sustainable Energy Rev.* **2017**, *70*, 399. [Crossref]
13. Jakeria, M. R.; Fazal, M. A.; Haseeb, A. S. M. A.; *Renewable Sustainable Energy Rev.* **2014**, *30*, 154. [Crossref]
14. Lima, A. S.; Silva, D. G.; Teixeira, L. S. G.; *Environ. Monit. Assess.* **2015**, *187*, 4122. [Crossref]
15. Antunes, G. A.; dos Santos, H. S.; da Silva, Y. P.; Silva, M. M.; Piatnicki, C. M. S.; Samios, D.; *Energy Fuels* **2017**, *31*, 2944. [Crossref]
16. Pereira, F. M.; Zimpeck, R. C.; Brum, D. M.; Cassella, R. J.; *Talanta* **2013**, *117*, 32. [Crossref]
17. Ghisi, M.; Chaves, E. S.; Quadros, D. P. C.; Marques, E. P.; Curtius, A. J.; Marques, A. L. B.; *Microchem. J.* **2011**, *98*, 62. [Crossref]
18. Azevedo Silva, J. S.; Chaves, E. S.; dos Santos, É. J.; Saint'Pierre, T. D.; Frescura, V. L. A.; Curtius, A. J.; *J. Braz. Chem. Soc.* **2010**, *21*, 620. [Crossref]
19. Mirceski, V.; Gulaboski, R.; Lovric, M.; Bogeski, I.; Kappl, R.; Hoth, M.; *Electroanalysis* **2013**, *25*, 2411. [Crossref]
20. Economou, A.; Kokkinos, C. In *Electrochemical Strategies in Detection Science*, 1<sup>st</sup> ed.; Arrigan, D. W. M., ed.; Royal Society of Chemistry: London, UK, 2015, ch. 1.
21. Osteryoung, J. G.; Osteryoung, R. A.; *Anal. Chem.* **1985**, *57*, 101. [Crossref]
22. Lovrić, M. In *Electroanalytical Methods: Guide to Experiments and Applications*, 2<sup>nd</sup> ed.; Scholz, F., ed.; Springer: Berlin, Germany, 2010, ch. II.3.
23. Mirceski, V.; Gulaboski, R.; *Maced. J. Chem. Chem. Eng.* **2014**, *33*, 1. [Crossref]
24. Borrill, A. J.; Reily, N. E.; Macpherson, J. V.; *Analyst* **2019**, *144*, 6834. [Crossref]
25. Economou, A.; Fielden, P. R.; *Analyst* **2003**, *128*, 205. [Crossref]
26. Vyskočil, V.; Barek, J.; *Crit. Rev. Anal. Chem.* **2009**, *39*, 173. [Crossref]
27. Shi, D.; Wu, W.; Li, X.; *Sens. Biosens. Res.* **2021**, *34*, 100464. [Crossref]
28. de Carvalho, L. M.; do Nascimento, P. C.; Koschinsky, A.; Bau, M.; Stefanello, R. F.; Spengler, C.; Bohrer, D.; Jost, C.; *Electroanalysis* **2007**, *19*, 1719. [Crossref]
29. de Oliveira, M. F.; Saczk, A. A.; Okumura, L. L.; Fernandes, A. P.; de Moraes, M.; Stradiotto, N. R.; *Anal. Bioanal. Chem.* **2004**, *380*, 135. [Crossref]
30. Carapuça, H. M.; Monterroso, S. C. C.; Rocha, L. S.; Duarte, A. C.; *Talanta* **2004**, *64*, 566. [Crossref]
31. Khoo, S. B.; Guo, S. X.; *Electroanalysis* **2002**, *14*, 813. [Crossref]
32. Fischer, E.; van den Berg, C. M. G.; *Anal. Chim. Acta* **1999**, *385*, 273. [Crossref]
33. dos Santos, G. F. S.; Ferreira, R. Q.; *Microchem. J.* **2020**, *156*, 104849. [Crossref]
34. Pinto, L.; Lemos, S. G.; *Microchem. J.* **2013**, *110*, 417. [Crossref]
35. Tormin, T. F.; Oliveira, G. K. F.; Richter, E. M.; Munoz, R. A. A.; *Electroanalysis* **2016**, *28*, 940. [Crossref]
36. Squissato, A. L.; Neri, T. S.; Coelho, N. M. M.; Richter, E. M.; Munoz, R. A. A.; *Fuel* **2018**, *234*, 1452. [Crossref]
37. Holmes, J.; Pathirathna, P.; Hashemi, P.; *TrAC, Trends Anal. Chem.* **2019**, *111*, 206. [Crossref]
38. Kokkinos, C.; Economou, A.; *Sens. Actuators, B* **2016**, *229*, 362. [Crossref]
39. Oldham, K. B.; *J. Electroanal. Chem. Interfacial Electrochem.* **1988**, *250*, 1. [Crossref]
40. Howell, J. O.; Mark Wightman, R.; *Anal. Chem.* **1984**, *56*, 524. [Crossref]
41. Vicentino, P. O.; Cassella, R. J.; *Talanta* **2017**, *162*, 249. [Crossref]
42. Vinhal, J. O.; Cassella, R. J.; *Spectrochim. Acta, Part B* **2019**, *151*, 33. [Crossref]
43. Vinhal, J. O.; Vicentino, P. O.; da Silva, P. K. A.; Cassella, R. J.; *Energy Fuels* **2019**, *33*, 3916. [Crossref]
44. Vicentino, P. O.; Cassella, R. J.; Leite, D.; Resano, M.; *Talanta* **2020**, *206*, 120230. [Crossref]
45. de Oliveira, G. C.; Vicentino, P. O.; Cassella, R. J.; Xing, Y. T.; Ponzio, E. A.; *Electroanalysis* **2021**, *33*, 682. [Crossref]
46. Moreira, L. F. P. P.; Beluomini, M. A.; de Souza, J. C.; Stradiotto, N. R.; *Electroanalysis* **2017**, *29*, 1941. [Crossref]
47. Kumar, H.; Sarma, A. K.; Kumar, P.; *Renewable Sustainable Energy Rev.* **2020**, *117*, 109498. [Crossref]
48. Leng, L.; Han, P.; Yuan, X.; Li, J.; Zhou, W.; *Energy* **2018**, *153*, 1061. [Crossref]
49. Rosen, M. J.; Kunjappu, J. T. In *Surfactants and Interfacial Phenomena*, 4<sup>th</sup> ed.; John Wiley & Sons: Hoboken, USA, 2012, ch. 1.
50. Babadagli, T.; Ozum, B.; *Soc. Pet. Eng.* **2010**, SPE-133376-MS. [Crossref]
51. Goberdhan, D. G. C.; Hunt, R.; *SAE Technical Papers* **2015**, *1*, 0907. [Crossref]
52. Agência Nacional do Petróleo, Gás Natural e Biocombustíveis (ANP); Nota Técnica No. 10/2021/SBQ-CPT-CQC/SBQ/ANP, de 13 de setembro de 2021, *Análise de Impacto Regulatório - Especificações Nacionais do Biodiesel (B100)*, section 115, p.14. [Link] accessed in November 2022
53. Sherigara, B. S.; Shivaraj, Y.; Mascarenhas, R. J.; Satpati, A. K.; *Electrochim. Acta* **2007**, *52*, 3137. [Crossref]

54. Ferreira, R.; Chaar, J.; Baldan, M.; Braga, N.; *Fuel* **2021**, *291*, 120104. [Crossref]
55. Wang, J.; *Stripping Analysis: Principles, Instrumentation, and Applications*; VCH Publishers: Deerfield Beach, USA, 1985.
56. Lovrić, M. In *Electroanalytical Methods: Guide to Experiments and Applications*, 2<sup>nd</sup> ed.; Scholz, F., ed.; Springer: Berlin, Germany, 2010, ch. II.7
57. Mirceski, V.; Komorsky-Lovric, S.; Lovric, M.; *Square-Wave Voltammetry: Theory and Application*; Springer: Berlin, Germany, 2007.
58. Ansari, R.; Kazi, T. G.; Jamali, M. K.; Arain, M. B.; Wagan, M. D.; Jalbani, N.; Afridi, H. I.; Shah, A. Q.; *Food Chem.* **2009**, *115*, 318. [Crossref]
59. Chaves, E. S.; dos Santos, E. J.; Araujo, R. G. O.; Oliveira, J. V.; Frescura, V. L. A.; Curtius, A. J.; *Microchem. J.* **2010**, *96*, 71. [Crossref]
60. Adeloju, S. B. O.; Pablo, F.; *Anal. Chim. Acta* **1992**, *270*, 143. [Crossref]
61. Adeloju, S. B. O.; Pablo, F.; *Anal. Chim. Acta* **1994**, *288*, 157. [Crossref]
62. Adeloju, S. B. O.; Pablo, F.; *Electroanalysis* **1995**, *7*, 476. [Crossref]
63. Baś, B.; *Anal. Chim. Acta* **2006**, *570*, 195. [Crossref]
64. Calvo-Pérez, A.; Domínguez-Renedo, O.; Alonso-Lomillo, M. A.; Arcos-Martínez, M. J.; *Electroanalysis* **2010**, *22*, 2924. [Crossref]
65. Ensafi, A. A.; Ring, A. C.; Fritsch, I.; *Electroanalysis* **2010**, *22*, 1175. [Crossref]
66. Grabarczyk, M.; Wasąg, J.; *J. Electrochem. Soc.* **2016**, *163*, H218. [Crossref]
67. Jagner, D.; Renman, L.; Stefansdottir, S. H.; *Anal. Chim. Acta* **1993**, *281*, 305. [Crossref]
68. lo Balbo, A.; Dall'Orto, V. C.; Sobral, S.; Rezzano, I.; *Anal. Lett.* **1998**, *31*, 2717. [Crossref]
69. Piech, R.; Baś, B.; Kubiak, W. W.; *Electroanalysis* **2007**, *19*, 2342. [Crossref]
70. Piech, R.; *Electroanalysis* **2013**, *25*, 716. [Crossref]
71. Yang, H. Y.; Sun, I. W.; *Anal. Chim. Acta* **1998**, *358*, 285. [Crossref]
72. Zen, J.-M.; Lee, M.-L.; *Anal. Chem.* **1993**, *65*, 3238. [Crossref]
73. Nagaosa, Y.; Zong, P.; Kamio, A.; *Microchim. Acta* **2009**, *167*, 241. [Crossref]
74. da Silva, O. B.; Machado, S. A. S.; *Anal. Methods* **2012**, *4*, 2348. [Crossref]
75. Coordenação Geral de Acreditação (INMETRO); *Orientação Sobre Validação de Métodos Analíticos, DOQ-CGCRE-008*, Revisão 08, de Abril de 2020. [Link] accessed in November 2022

Submitted: September 7, 2022

Published online: November 16, 2022

